Cell Stress and Chaperones (2017) 22:15–27
DOI 10.1007/s12192-016-0736-y

ORIGINAL PAPER

Ultrastructural and physiological changes induced by different stress conditions on the human parasite *Trypanosoma cruzi*

Deyanira Pérez-Morales[1] · **Karla Daniela Rodríguez Hernández**[1] · **Ignacio Martínez**[1] · **Lourdes Teresa Agredano-Moreno**[2] · **Luis Felipe Jiménez-García**[2] · **Bertha Espinoza**[1]

Received: 22 August 2016 / Accepted: 12 September 2016 / Published online: 6 October 2016

Abstract *Trypanosoma cruzi* is the etiological agent of Chagas disease. The life cycle of this protozoan parasite is digenetic because it alternates its different developmental forms through two hosts, a vector insect and a vertebrate host. As a result, the parasites are exposed to sudden and drastic environmental changes causing cellular stress. The stress response to some types of stress has been studied in *T. cruzi*, mainly at the molecular level; however, data about ultrastructure and physiological state of the cells in stress conditions are scarce or null. In this work, we analyzed the morphological, ultrastructural, and physiological changes produced on *T. cruzi* epimastigotes when they were exposed to acid, nutritional, heat, and oxidative stress. Clear morphological changes were observed, but the physiological conditions varied depending on the type of stress. The maintenance of the physiological state was severely affected by heat shock, acidic, nutritional, and oxidative stress. According to the surprising observed growth recovery after damage by stress alterations, different adaptations from the parasite to these harsh conditions were suggested. Particular cellular death pathways are discussed.

Keywords *Trypanosoma cruzi* · Stress · Physiological damage · Apoptosis

Introduction

Chagas Disease is a major endemic problem in Latin America caused by the flagellated protozoa *Trypanosoma cruzi*. This parasitic disease affects about 8 million people in the region (WHO 2015). Seroprevalence of more than two million people and an incidence of 72,677 new cases were calculated for Mexico and Central America (WHO 2015). In addition, the migration of people from Latin America to USA, Canada, many European, and some Western Pacific countries has been a factor for the spreading of the disease to the rest of the world.

T. cruzi is a protozoan parasite with a complex digenetic life cycle, showing three main morphological stages: metacyclic trypomastigote in the insect hindgut, blood trypomastigote in the blood of mammals, epimastigote inside the vector intestine and amastigote the intracellular stage in mammals. Each of these stages will overcome hostile environments and suffer from different types of stress (Requena et al. 1992). The parasite will confront different pH, temperature, oxidative stress, and nutrient availability, among other stress conditions. Thus, the parasites display an adaptive response (physiological, genetic, or epigenetic) to counter these stress conditions.

Currently, two main types of stress are recognized: abiotic and biotic (Thammavongs et al. 2008). *T. cruzi* will suffer from both stress: the epimastigote stage, localized in the vector intestine, will confront the presence of the immune response of the invertebrate and a temperature of 28 °C. Furthermore, starvation will induce stress. This nutritional stress in the vector will induce different developmental stages in the parasite;

Electronic supplementary material The online version of this article (doi:10.1007/s12192-016-0736-y) contains supplementary material, which is available to authorized users.

✉ Bertha Espinoza
besgu@iibiomedicas.unam.mx

[1] Laboratorio de Estudios sobre Tripanosomiasis. Departamento de Inmunología, Instituto de Investigaciones Biomédicas, Universidad Nacional Autónoma de México, A.P. 70228, C.P. 04510 Ciudad de México, México

[2] Departamento de Biología Celular, Facultad de Ciencias, Universidad Nacional Autónoma de México, A.P. 70228, C.P. 04510 México, D.F., México

in particular, the lack of food will induce the transformation of epimastigote to trypomastigote (Contreras et al. 1985; Kollien and Schaub 1998). Also inside the vector intestine, the parasite will contend with variable pH from 5.7 to 8.9, depending on the amount of food ingested by the vector (Kollien et al. 2001). The epimastigote stage will also face oxidative stress produced by the metabolites of the hemoglobin ingested by the vector during its meals (Nogueira et al. 2015). When the amastigote stage is in the intracellular mammalian environment, the parasite will encounter an acidic pH inside the parasitophorous vacuole (Hall 1993). Furthermore, this intracellular stage will have to face the oxidative stress as a result of the immune mechanisms of macrophages and other immune cells. The metacyclic trypomastigote, the infective mammalian stage, will meet the immune response of the host and a temperature range of 36–38 °C. The oxidative stress will be present in all parasite stages of the life cycle, since the immune response of the vertebrate and invertebrate hosts will be the main origin of this kind of stress. The mammal hosts produce different types of reactive oxygen species (ROS) as a consequence of the activation of the enzyme NADPH oxidase inside the activated macrophages. During the phagocytosis, this enzyme produces high quantities of superoxide radical ($O_2^{\cdot-}$), which will dismutate to H_2O_2 or react with iNOS-derived nitric oxide (NO) to yield peroxynitrite ($ONOO^-$), a reactive nitro species (RNO), which is a strong oxidant and a potent cytotoxic effector molecule against *T. cruzi*. Furthermore, in the presence of metallic ions, H_2O_2 generate the highly reactive hydroxyl ($^{\cdot}OH$) radical (Piacenza et al. 2013).

In the case of the invertebrate vector, the production of antimicrobial peptides has been reported as part of the immune response against microorganisms, as well as the induction of melanization and encapsulation, which are associated with the production of ROS and RNO (Castillo et al. 2011).

It is important to mention that the different types of stress can also produce oxidative stress with the presence of ROS, as has been reported for immune and thermal stress (Weis 2008). These phenomena will induce apoptosis and/or necrosis.

Apoptosis is a type of programmed cell death found in metazoan organisms, and its role in protozoans is controversial. It is highly conserved and it is a critical process in tissue morphogenesis and homeostasis and in the elimination of damaged cells (Raff 1998; Weis 2008). It is characterized by an orderly proscribed set of events leading to cell death. Once the cascade is initiated, morphological alterations include cell shrinkage, fragmentation of DNA, condensation of chromatin, and the formation of apoptotic bodies that contain packaged cellular debris.

In contrast to apoptosis, necrosis is uncontrolled cell death that is most often triggered by extrinsic factors that make the cell and its contents to swell, eventually causing rupture of the plasma membrane and release of cell material (Wyllie et al. 1980). It lacks both the distinctive morphological signature of apoptosis, such as condensed chromatin and apoptotic bodies, as well as a molecular signature such as execution by a suite of genes and pathways.

Furthermore, autophagy is believed to have arisen as a response to starvation and stress in the unicellular organisms, and the machinery to produce it is conserved from unicellular to mammalian cells. In *T. cruzi*, the presence of all components of the ubiquitin-like protein Atg8 conjugation system has been reported (Alvarez et al. 2008).

Separate reports on the effects of stress on the morphology of the parasite have been published but with many variants (parasite strain, type of stress, stress duration, etc.). Thus, it has been difficult to evaluate the morphological and physiological damage produced by stress. In this work, morphological and ultrastructural description, as well as changes in the physiological and growth capacity of *T. cruzi* as a result of different types of stress, is studied. Discussion on the evident resistance to several types of stress is included.

Materials and methods

Parasites

Epimastigotes of *T. cruzi* Queretaro strain (Tc-I) (TBAR/MX/0000/Queretaro) (Espinoza et al. 2010) were cultured at 28 °C in liver infusion tryptose (LIT) medium (Chiari and Camargo 1984), pH 7.2, supplemented with 10 % heat-inactivated fetal bovine serum (GIBCO) and 5 μg ml^{-1} hemine (Sigma). To reduce the experimental variability, the cultures were routinely kept in the exponential growth phase (30×10^6 cells ml^{-1}), and this amount of parasites was reached after 3 days of culture.

Stress conditions

Cultures of 10 ml of LIT medium containing epimastigotes in the exponential growth phase were divided in equal volumes and washed three times for centrifugation with phosphate-buffered saline (PBS), and finally, two pellets were obtained. One of the pellets was resuspended in 5 ml of fresh LIT medium and grown at 28 °C (except for heat stress, see below) for 2, 3, or 24 h as indicated, and it represented the control condition. The other pellet was resuspended in 5 ml of the specific medium to induce cellular stress.

Acid stress was provoked by growing the parasites in LIT medium buffered at pH 5.0 at 28 °C for 3 or 24 h.

Growing of the epimastigotes in triatomine artificial urine (TAU) medium (190 mM NaCl, 8 mM phosphate buffer pH 6.0, 17 mM KCl, 2 mM $CaCl_2$, 2 mM $MgCl_2$) (Contreras et al. 1985) at 28 °C for 3 or 24 h induced a nutritional stress.

Heat shock was produced when the parasites were grown in LIT medium at 39 °C in a temperature controlled incubator for 3 or 24 h.

Oxidative stress was induced by exposing the parasites to 160 μM H_2O_2 in incubation buffer (5 mM KCl, 80 mM NaCl, 2 mM $MgCl_2$, 16.2 mM Na_2HPO_4, 3.8 mM NaH_2PO_4, 0.15 % bovine serum albumin) (Carnieri et al. 1993) at 28 °C for 2 h.

After each incubation period (2, 3, or 24 h), an aliquot from the culture was taken to evaluate morphology, motility, viability, mitochondrial membrane potential, the type of cell death (apoptosis or necrosis), and recovery of the growth. The culture remainder was harvested by centrifugation at 2,500×*g* for 10 min at 4 °C and washed three times with PBS. The obtained pellets were processed for ultrastructural analysis.

Light microscopy

To observe changes in cell morphology, permanent microscopic preparations of untreated and treated parasites were made. Twenty microliters of the corresponding culture were spread onto a well of a teflon printed slide (Electron Microscopy Sciences), air dried for 20 min at room temperature, dehydrated in methanol for 5 min, and stained with Giemsa (Sigma) for 15 min. Then, the slides were washed in water, air-dried, and mounted in organo/limonene mount resin (Santa Cruz Biotechnology) with a coverslip. The slides were observed in a Nikon Optiphot 2 light microscope coupled with a Nikon Coolpix 4300 digital camera. Several images were acquired and at least 100 cells were counted in each independent experiment. The number of normal or abnormal cells versus the total number of cells was determined and expressed as percentage.

Calculations of the cellular area were obtained from digital analysis using ImageJ software (image processing and analysis in Java), version 1.48 (National Institutes of Health, USA) (http://imagej.nih.gov).

The parasite motility was evaluated by visual inspection of fresh smears in a Neubauer hemocytometer using a light microscope at 2, 3, or 24 h of exposure in control and stress conditions, and the number of motile cells versus the total number of cells was determined and expressed as percentage of motile cells. In control conditions, we observed that the parasites were swimming continuously, the absence of any motion was considered as immobility.

Transmission electron microscopy

To evaluate the ultrastructure of the parasites, we used standard transmission electron microscopy (TEM) (Jiménez-García and Segura-Valdéz 2004). Briefly, the samples were fixed in a mixture of 4 % paraformaldehyde/2.5 % glutaraldehyde in PBS for 3 h, washed in PBS, post-fixed in 1 % osmium tetroxide for 2 h, washed with PBS, dehydrated for incubating in a graded series of ethanol (30, 50, 70, 80, 90, 96, and 100 %), incubated in propylene oxide, and then embedded in propylene oxide/epoxy resin (1:1) for 18 h and finally incorporated in Eppendorf microtubes and polymerizated at 60 °C for 48 h. Ultrathin sections of 40–60 nm were mounted on formvar coated copper grids and contrasted with 5 % uranyl acetate and 0.5 % lead citrate for 20 and 10 min, respectively. The samples were photographed in a transmission electron microscope (JEOL 1010, JEOL, Peabody, MA) operating 80 kV.

Viability assay

The viability of *T. cruzi* epimastigotes Qro strain was determined using LIVE/DEAD Viability/Cytotoxicity Kit (3224, Molecular Probes) (Sandes et al. 2014). For this, 2×10^6 parasites ml^{-1} during the exponential growth phase were incubated at 28 °C in 24 well plates and subjected to different types of stress. After the indicated incubation time, the parasites were centrifuged at 342×*g* for 10 min to remove the supernatant medium, and the pellet of parasites of each treatment was resuspended in 997 μl of PBS, 4 μl of a solution of Calcein-AM (C-AM) 50 mM, and 1 μl of ethidium homodimer (EthD-1) 2 mM. The samples were then incubated for 20 min at room temperature and immediately analyzed in a flow cytometer (BD FACSCalibur flow cytometer) with a 530/30-nm filter (FL1-H) for calcein (green fluorescence/ living cells) and a 488/10-nm filter (FL2-H) for EthD-1 (red fluorescence/dead cells), and 15,000 events per treatment were acquired. The data were analyzed using FlowJo 7.3.2 software and expressed as the percentage of cells for each population phenotype. The compensation was performed using live parasites grown in medium alone and stained only with C-AM and dead parasites exposed to heat shock (55 °C for 15 min) and stained with EH. Three independent experiments by duplicate were done.

MTT reductase activity assays

Epimastigotes (2×10^7 cells ml^{-1}) were subjected to different types of stress as mentioned above and after that, they were centrifuged at 2,500×*g* during 10 min. Then, two washes by centrifugation were done using sterile PBS. Pellets were suspended in 300 μl of noncomplete LIT medium (without hemin and FBS) containing tetrazolium dye (MTT 3-(4,5-dimethyl-2-thiazolyl)-2,5-diphenyl-2H-tetrazolium bromide (0.5 mg/ml) and incubated at 28 °C during 4 h in dark. Parasites were recovered by centrifugation and supernatant was discarded. Formazan salt was dissolved in 170 μl of isopropanol by shaking during 15 min at room temperature. Fifty microliters of each sample were seeded for triplicate in 96-well plate round bottom, and absorbance was determinate at 595 nm with reference of 655 nm in a microplate reader

(550, Bio-Rad) (Grela et al. 2015). Samples were assayed in triplicate in three independent assays, and reductase activity percentage was determined comparing with total activity in control group nonstressed.

Mitochondrial membrane potential assay (ΔΨm)

After exposure to different types of stress, parasites (2×10^6 cells ml^{-1}) were centrifuged twice at 3,421×*g*, resuspended in 0.5 ml PBS with 10 μg/ml Rho 123 (Sigma-Aldrich, cat R8004-Sigma), and incubated for 20 min (Lazarin-Bidóia et al. 2013, 2016; Sandes et al. 2014; Volpato et al. 2015). The carbonyl cyanide 3-chloro phenylhydrazone (CCCP) 100 μM (Sigma-Aldrich) was used as positive control. Then, the parasites were washed in PBS as described above and immediately analyzed using a FACSCalibur flow cytometer equipped whit CellQuest software, and the fluorescence intensities for Rho 123 (mitochondrial membrane potential) were quantified. A total of 20,000 events were acquired in the region previously established as corresponding to *T. cruzi* epimastigotes, based on the forward (FSC) and side (SSC) scatter. Alterations in the fluorescence intensities of Rho 123 (FL1-H) were quantified by the index of variation that was obtained by the equation (TM − CM)/CM, where TM is the median of fluorescence for treated parasites and CM is the median of fluorescence for control parasites (nontreated). Negative index of variation values corresponds to the depolarization of the mitochondrial membrane, which is an established feature of apoptotic cells.

Cell death assay

To determine if the parasites subjected to different types of stress died by necrosis or apoptosis, the Annexin V/Dead Cell Apoptosis Kit (V13241, Molecular Probes) was used (Lazarin-Bidóia et al. 2013). For this, *T. cruzi* epimastigotes were exposed to different types of stress as describe above. The antibiotic Antimycin A (AA; 187.5 μM) was used as a positive control, since this antibiotic has been reported to induce apoptosis in this parasite. After the indicated incubation time, the parasites (2×10^6 cells ml^{-1}) were centrifuged at 3421×*g* for 10 min, and the pellet was washed with PBS and resuspended in 493.5 μl of binding buffer annexin-V (50 mM HEPES, 700 mM NaCl, 12.5 mM $CaCl_2$, pH 7.4), 5 μl of a solution of annexin V (AV-FITC), and 1.5 μl of a solution of propidium iodide (PI) 1.5 mM. Samples were incubated for 20 min at room temperature and immediately analyzed in a flow cytometer (same as mentioned above) with a 530/30-nm filter (FL1-H) for Annexin V-FITC (green fluorescence/apoptotic cell) and a filter <575 nm (FL3-H) for PI (red fluorescence/necrotic cells), and 15,000 events for each treatment were acquired. The data were analyzed using FlowJo 7.3.2 software and expressed as the percentage of cells in each population phenotype. The compensation was performed using cultured parasites with AA antibiotic and stained only with AV-FITC and heat-killed parasites (as described above) and stained with PI. Three independent experiments by duplicate were done.

Parasites growth recovery

Epimastigotes (2×10^6 cells ml^{-1}) control or stressed (for 2 or 24 h as indicated in each type of stress) were washed, reinoculated in fresh LIT medium, and after 48 h, the number of parasites was determined by counting in a hemocitometer. The number of control parasites was considered as 100 % of growth. Three independent experiments were done.

Statistical analysis

Data from the determination of the cellular area and the relative rate of growth between untreated and treated parasites were analyzed by paired *t* tests with a 95 % confidence interval using GraphPad Prism 5 program version 5.04 (GraphPad Software, san Diego, CA). For the MTT assay, statistical differences were determined by one-way ANOVA of independent samples, using Vassar Stats Software (Vassar College, Poughkeepsie, NY). For ΔΨm assays, statistical differences were determined by one-way ANOVA and a Dunnett's multiple comparison tests using also GraphPad Prism 5 program version 5.04.

Results

Morphological changes in *T. cruzi* epimastigotes after stress treatment

As a first approach, we evaluated the effect of acid, nutritional, oxidative, and heat stress on the morphology of epimastigotes of *T. cruzi*. For that, we incubated the parasites in LIT broth at 28 °C (control conditions), in LIT buffered at pH 5.0 (acidic stress), in TAU medium (nutritional stress), in the presence of 160 μM H_2O_2 (oxidative stress) or at 39 °C (heat shock) for different time periods. When observed by light microscopy, *T. cruzi* epimastigotes grown in control conditions for 3 and 24 h exhibited the typical morphology with an elongated body, terminal flagellum, and the nucleus and kinetoplastid in the usual position (Fig. 1a, e). In contrast, epimastigotes exposed to acidic stress for 3 h showed significant morphological changes, which included contortion or shrinkage of the parasite body (Fig. 1b, Table 1), and after 24 h, the body contraction was accentuated and almost all parasites acquired a rounded appearance, some with a shortened flagellum and others lacking this organelle (Fig. 1f, Table 1).

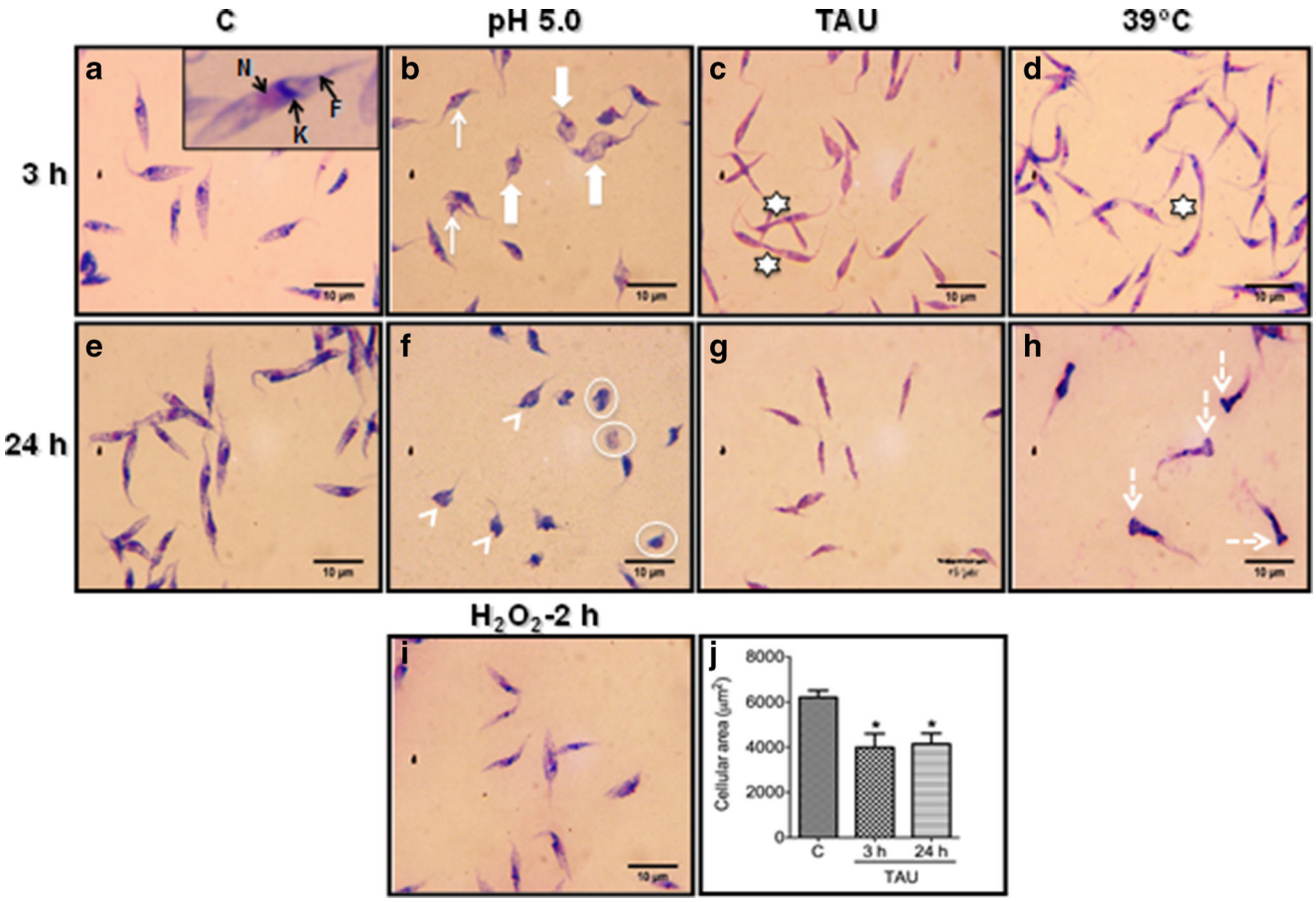

Fig. 1 Representative micrographs showing the cellular shape of *Trypanosoma cruzi* epimastigotes subjected to different types of stress. In **a** and **e**, Giemsa stained smears of control epimastigotes showing a typical elongated cell shape. **a** Close up of an epimastigote exhibiting nucleus (*N*), kinetoplast (*K*), and flagellum (*F*). × Parasites exposed to acid stress for 3 h show a contortion (*arrow*) or shrinkage (*thick arrow*) of the parasite body and **f** parasites exposed for 24 h, the parasites body showed rounded shape (*arrowhead*), and some of them lacks flagellum (*enclosed in a circle*). **c**, **g** Epimastigotes subjected to nutritional stress for 3 or 24 h shows a typical elongated morphology but with a slimmer appearance. **d** Epimastigotes exposed to heat shock for 3 h exhibit a normal morphology and **h** at 24 h shows a pronounced swelling in the posterior region of the body (*dotted arrow*). **i** After oxidative stress for 2 h, the parasites do not show any alteration in their morphology. **j** Parasite cellular area in control and nutritional stress conditions determined with the ImageJ program. At least 150 parasites were measured in each condition (*$P < 0.05$). The stars in **c** and **d** indicate dividing parasites. As a minimum five independent experiments were performed for each condition, showing similar results

When the parasites were exposed to nutritional stress for 3 and 24 h, they showed a typical elongated morphology, but they look slimmer than the parasites in control conditions (Fig. 1c, g, Table 1). To support this observation, we measure the cellular area of the parasites in control and stress conditions using ImageJ software. Control parasites had an average cellular area of 6,000 μm^2, and this decreased significantly to about 4000 μm^2 in the nutritionally stressed parasites (Fig. 1j).

When the parasites were exposed to heat shock for 3 h, they displayed a normal shape (Fig. 1d, Table 1), but after 24 h, they acquired an abnormal form, as a pronounced swelling in the posterior region of the body was evident in the bulk of the parasites (Fig. 1h, abnormal in Table 1).

In *T. cruzi* epimastigotes exposed to oxidative stress for 2 h, no evident alteration in the morphology was observed by light microscopy (Fig. 1i), but interestingly, only for this type of stress the motility of the parasites, which could be easily evaluated in fresh smears at the light microscope, was severely affected, since about 80 % of the parasites were immobilized, compared with the control parasites, which displayed a percentage of motility of 98–100 %.

Ultrastructural and physiological alterations in *T. cruzi* epimastigotes after stress treatment

In order to get more evidence about the effect of different types of stress on *T. cruzi* epimastigotes, we used TEM to analyze the ultrastructural changes on the cells. For these analyses, we chose the longest time of incubation in stress conditions, i.e., 24 h (with the exception of oxidative stress), because at this incubation time, we observed the most dramatic morphological changes, suggesting a significant effect on

Table 1 Cell shape of epimastigotes subjected to different stress conditions

	Cell shape				
	Normal	Contorted	Rounded	Rounded aflagellate	Abnormal
Treatment 3 h					
Control	100	0	0	0	0
Acidic stress	0	88.31 ± 13.35	8.66 ± 3.51	0	0
Nutritional stress[a]	100	0	0	0	0
Heat shock	100	0	0	0	0
Oxidative stress	100	0	0	0	0
Treatment 24 h					
Control	100	0	0	0	0
Acidic stress	0	0	39.67 ± 5.03	50.66 ± 16.80	0
Nutritional stress[a]	100	0	0	0	0
Heat shock	24.33 ± 6.65	0	0	0	73.05 ± 2.65

For each treatment, the number of normal or abnormal cells versus the total number of cells was determined by light microscopy as described in "Materials and methods" and expressed as percentage. The numbers denote mean and standard deviation of at least five independent experiments.

parasites biology. For oxidative stress, we determined 2 h to evaluate the possible ultrastructural alterations according to the mobility data, and because with this type of stress, longer incubation times produced parasite lysis.

The TEM analysis of *T. cruzi* epimastigotes exposed to acidic stress are shown in Fig. 2. The ultrastructure of untreated parasites exhibited organelles with a typical morphology distinctive of epimastigotes as was described by de Souza (2009), which include the unique and highly branched mitochondrion; the kinetoplast that appears like an elongated and electron dense structure that is made of a particular DNA (kDNA) and is located within the mitochondrial matrix; a nucleus that displays condensed chromatin adjacent to the nuclear envelope; and the nucleolus, a spherical intranuclear organelle (Fig. 2a (a)). In contrast, when the parasites were exposed to pH 5.0, significant ultrastructural alterations were observed, mainly related to severe kinetoplast-mitochondrion complex damage, such as a prominent mitochondrial swelling accompanied by a loss in density of the mitochondrial matrix and reduction of kDNA compaction (Fig. 2a (b, c, d, f)). In addition, acidic stress also induced the dilatation of Golgi complex cisternae (Fig. 2a (d)), abnormal distribution of nuclear chromatin (Fig. 2a (c, d)), and reduction of the nucleolus (Fig. 2a (c, d, e)).

Surprisingly, the majority of the parasites remained alive (97.20 ± 3.12 %), as indicated by the LIVE/DEATH assay that showed esterase activity by enzymatic conversion of nonfluorescent cell-permeant calcein to highly florescent calcein in the alive parasites. Few parasites showed membrane damage (6.24 ± 3.16 %) as determined by the incorporation of EthD-1 in the DNA of the cells (Fig. 2b). To support these results, a MTT assay to evaluate viability through enzyme activity was also performed and the reductase activity was 77 ± 2.42 %. This indicates that most of the cells remain with metabolic activity.

The mitochondrial membrane potential ($\Delta\Psi m$) was evaluated, and the results showed a moderate reduction on the total Rh123 fluorescence intensity indicated by the variation index of −0.39 ± 0.06 with respect to the control no treated ($P \leq 0.05$) (Fig. 2c). Even that, the apoptosis/necrosis assay was negative, since only few of the parasites suffered apoptosis or necrosis (6.31 %) (Fig. 2d).

In *T. cruzi* epimastigotes exposed to nutritional stress, the ultrastructural changes involved alterations in the mitochondrion-kinetoplast region, including a slight swelling of mitochondrion (Fig. 3a (b, d, e, f)) with the formation of intramitochondrial membranes (Fig. 3a (e, f)) and the loss of kDNA compaction (Fig. 3a (b, e, f)). Additionally, in the cytoplasm of the parasites, the accumulation of vesicles (Fig. 3a (b, e)) and the presence of multiple vacuoles (Fig. 3a (c, g)) were revealed. Importantly, some of these vacuoles were similar to autophagosomes because they appeared to contain inner concentric membranes (Fig. 3a (c, g)). Besides, no nucleus was evident in these parasites (Fig. 3a (b–g)).

Here again, most of the parasites were metabolically active (82.17 ± 7.54 %) and only 17.53 ± 7.33 % were dead as determined by the calcein/EthD-1 assay (Fig. 3b). But only 36 ± 2.15 % reductase activity was observed (Fig. 3b). A reduction on $\Delta\Psi m$ was observed in this condition, but this change was not significant (Fig. 3c). Most of the parasites were negative in the annexin V-PI assay and only 5.16 ± 4.01 % were suffering early or late apoptosis and 3.58 ± 2.13 % necrosis (Fig. 3d).

When the parasites were exposed to heat shock, one of the most evident finding was the presence of electron-dense fibrillar patches in the cytoplasm, which resembling stress granules

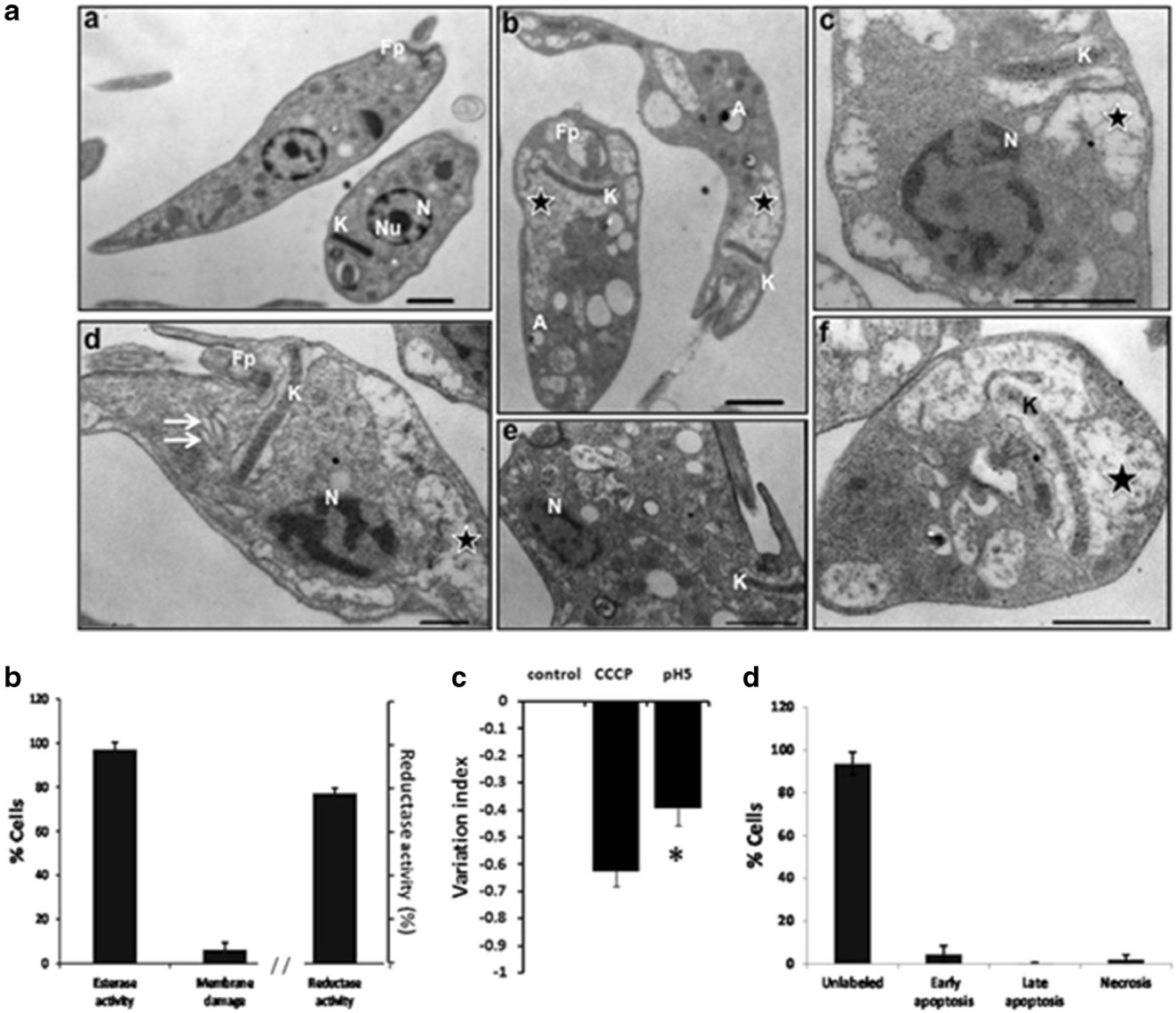

Fig. 2 Effects of acid stress on epimastigotes. **a** Representative transmission electron micrographs of *Trypanosoma cruzi* epimastigotes treated with acid stress (pH 5) for 24 h. **A** Control parasites showing normal morphology of nucleus (*N*), nucleolus (*Nu*), kinetoplastid (*K*) and flagellar pocket (Fp) (*a*). **A** Acid stress induces mitochondrial swelling and loss in density of the mitochondrial matrix (*b*, *c*, *d*, *f*, *star*), reduction of kDNA (*b*, *c*, *d*, *f*, *K*), dilatation of Golgi complex cisternae (*d*, *double arrow*), abnormal distribution of nuclear chromatin (*c*, *d*, *N*), and disappearance of the nucleolus (*c*, *d*, *e*). In **a** acidocalcisomes were observed (white A) (*b*). **b** Esterase activity and plasma membrane integrity determined by LIVE/DEAD viability/cytotoxicity Kit (Molecular Probes) in 2×10^6/mL epimastigotes after incubation with acid stress for 24 h. Reductase activity determined by MTT assay. **c** Mitochondrial membrane potential assay ($\Delta\Psi$m) was assayed with Rho 123 by flow cytometry using as positive control carbonyl cyanide 3-chloro phenylhydrazone (CCCP) and parasite no stressed as negative control. **d** Apoptosis and necrosis assayed by flow cytometry using FITC Annexin V/Dead cell Apoptosis kit (Invitrogen). **b**–**d** result from three independent experiments. $^{**}P < 0.01$, $^{*}P < 0.05$. *Bar* = 1 μm

(Fig. 4a (d–h)). An extensive vacuole development was also revealed in the parasite's cytoplasm (Fig. 4a (c, g, h, j)). Additionally, the mitochondrion appeared to be affected, because a mild swelling of this organelle was observed (Fig. 4a (i, k)). Heat-shocked parasites also showed the bleb formation over the plasma membrane (Fig. 4a (c, d, g)). Inside the nuclei, no nucleolus was detected (Fig. 4a (e, i)). The ultrastructure of these stressed parasites also suggested an arrest in cell growth because replicated organelles were detected, among these, duplicated axonemal microtubules (Fig. 4a (j)) and in another cell, two nuclei with only one kinetoplast (Fig. 4a (k)).

Results of EthD-1 incorporation into DNA showed that 84.87 ± 26.04 % of the parasites had plasma membrane damage and only 15.11 ± 12.89 % presented esterase activity (Fig 4b). Reductase activity was 66 ± 13 % (Fig. 4b). The parasites showed an important change in $\Delta\Psi$m value of

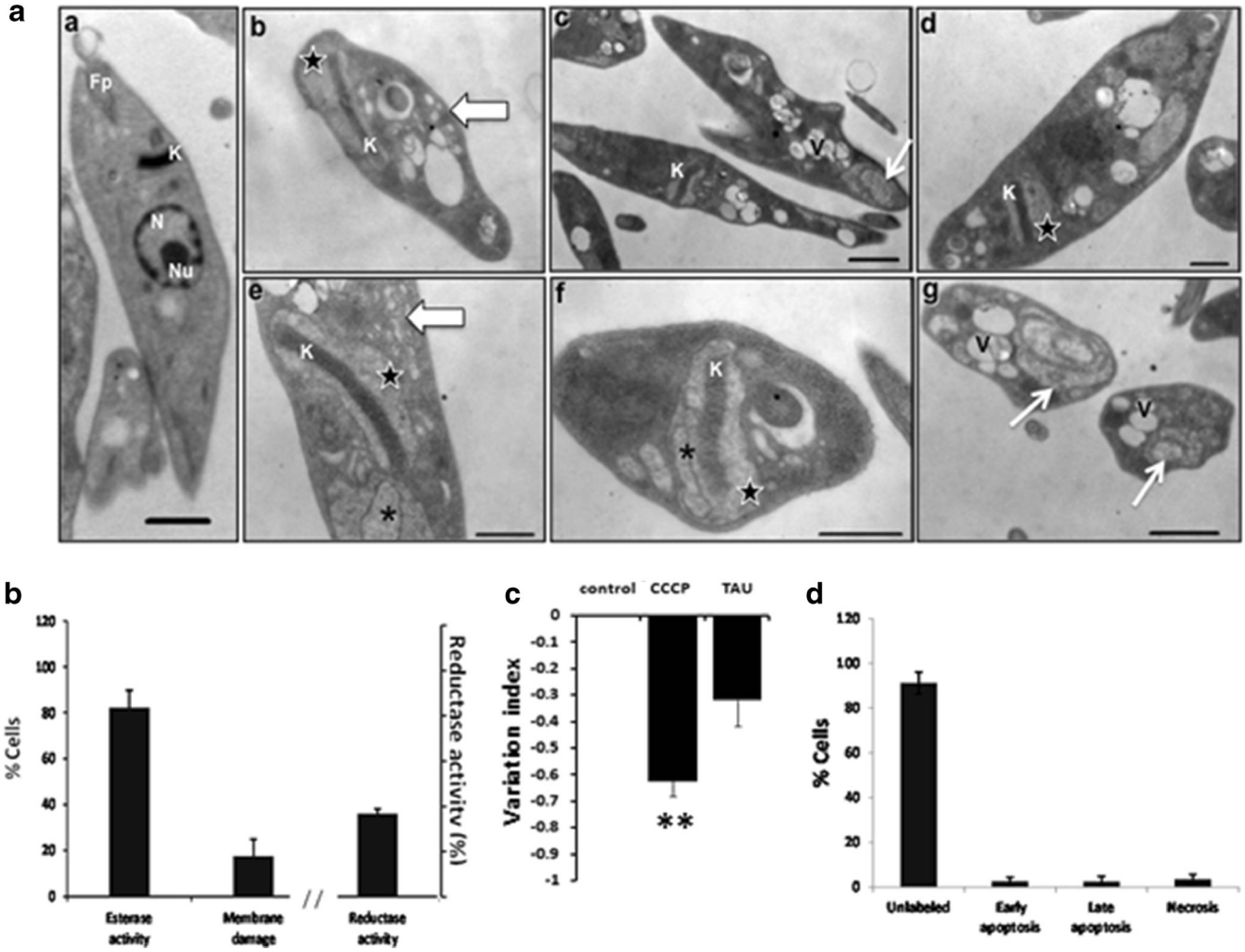

Fig. 3 Effects of nutritional stress on epimastigotes. **a** Representative transmission electron micrographs of *Trypanosoma cruzi* epimastigotes subjected to nutritional stress (TAU medium) for 24 h. **a** untreated parasites exhibit normal nucleus (*N*), nucleolus (*Nu*), kinetoplastid (*K*), and flagellar pocket (*Fp*). **a** The ultrastructural changes after stress include a slight swelling of mitochondria (*b*, *d*, *e*, *f*, *star*), development of intra-mitochondrial membranes (*e*, *f*, *asterisk*), loss of kDNA (*K*) compaction (*b*, *e*, *f*), cytoplasmic accumulation of vesicles (*b*, *e*, *thick arrow*), formation of multiple vacuoles (*c*, *g*, *V*), the presence of vacuoles with inner concentric membranes (*c*, *g*, *thin arrow*), and absence of nucleus (*b*–*g*). **b** Esterase activity and plasma membrane integrity determined by LIVE/DEAD viability/cytotoxicity Kit (Molecular Probes) in 2×10^6/mL epimastigotes after incubation with TAU medium for 24 h. Reductase activity determined by MTT assay. **c** Mitochondrial membrane potential assay ($\Delta\Psi$m) was assayed with Rho 123 by flow cytometry using carbonyl cyanide 3-chloro phenylhydrazone (*CCCP*) as positive control and nonstressed parasites as negative control. **d** Apoptosis and necrosis assayed by Flow cytometry using FITC Annexin V/Dead cell Apoptosis kit (Invitrogen). **b**–**d** result from three independent experiments. $^{**}P < 0.01$. *Bar* = 1 μm

-0.85 ± 0.06 (with a $P \leq 0.001$) with respect to nontreated parasites, which was higher than this observed with CCCP (Fig. 4c).

The damaged parasites were in early/late apoptosis or necrosis in the same numbers (around 4 %) (Fig. 4d).

The photomicrographs of parasites exposed to oxidative stress revealed that the main alteration in the ultrastructure was an abnormal distribution of chromatin and lacking of nucleolus (Fig. 5a (c–e)) and the appearance of blebs in plasma membrane (Fig. 5a (d–f)). A swelling of the mitocrondria membrane was also observed (Fig. 5a (b, e)).

When the esterase activity and the DNA incorporation of EthD-1 were assayed, it was observed that only 53.47 $\pm$ 25.52 % presented esterase activity and 46.39 $\pm$ 25.52 % presented membrane damage. The reductase activity was 49 $\pm$ 11.87 % (Fig. 5b). The $\Delta\Psi$m was significantly affected because the stressed parasites showed a strong reduction of -0.60 ± 0.20 similar to the value of the CCCP positive control with a $P \leq 0.01$ (Fig. 5c). In these experiments, the parasites were dyeing by early apoptosis (76.87 $\pm$ 4.28 %) and late apoptosis (16.47 $\pm$ 3.26 %) (Fig. 5d).

Parasite growth recovery after stress treatments

With the aim to relate the ultrastructural and metabolic damage produced as a consequence of stress treatment with

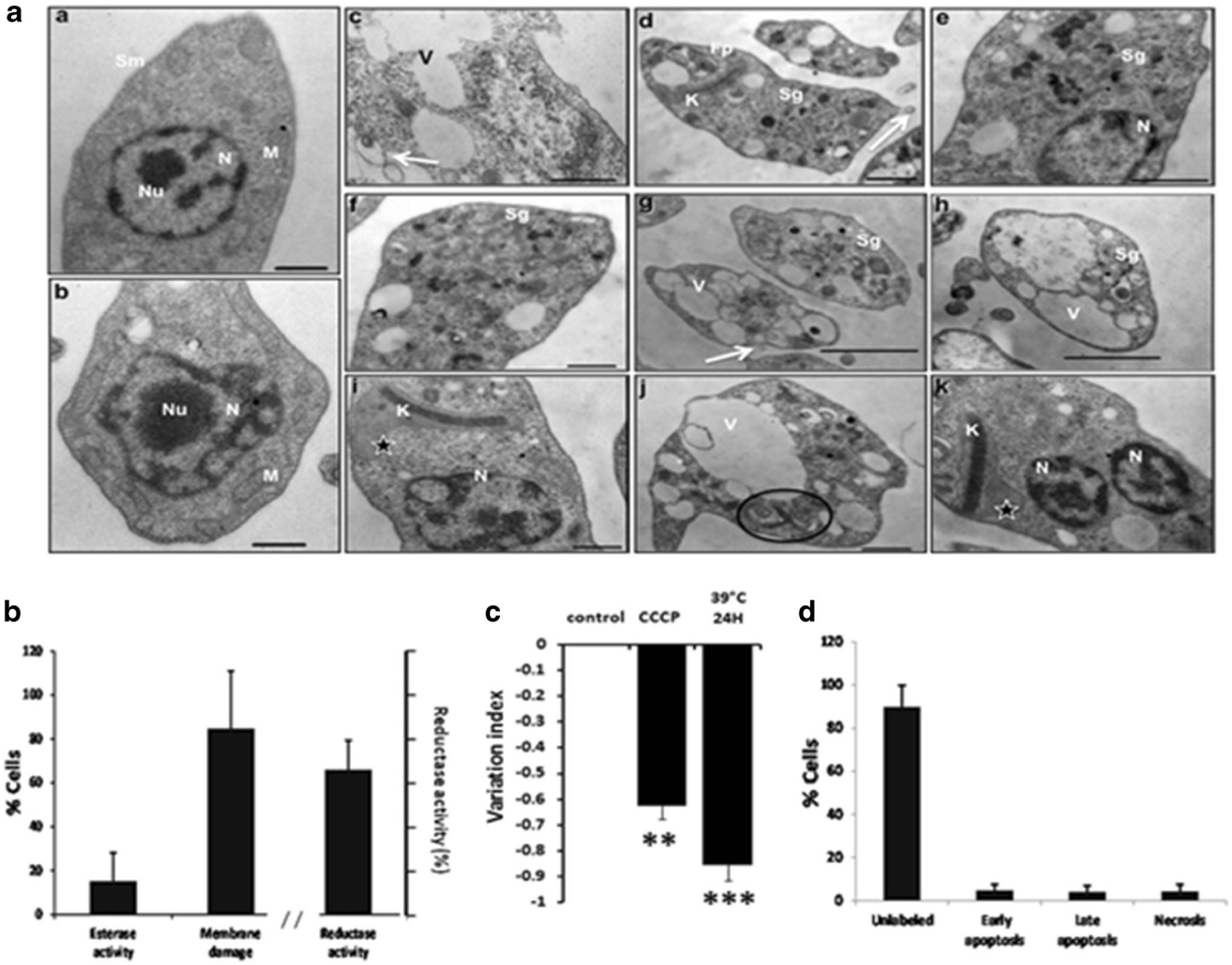

Fig. 4 Effects of heat shock on epimastigotes. **a** Representative transmission electron micrographs of *Trypanosoma cruzi* epimastigotes treated with heat shock (39 °C) for 24 h. **a** Control parasites showing well-preserved nucleus (*N*), nucleolus (*Nu*), and mitochondria (*M*) (*a* and *b*). **a** Stress induces alterations like the formation of electron dense fibrillar patches in the cytoplasm (*d–h*, *Sg*), development of prominent vacuoles in the cytoplasm (*c*, *g*, *h*, *j*, *V*), swelling of the mitochondria (*i*, *k*, *star*), bleb formation over the plasma membrane (*c*, *d*, *g*, *arrow*), absence of nucleolus (*e*, *i*), presence of duplicated axonemal microtubules (*j*, *circle*), and presence of two nuclei with only one kinetoplast (*N*, *K*) (*k*). **b** Esterase activity and plasma membrane integrity determined by LIVE/DEAD viability/cytotoxicity Kit (Molecular Probes) in 2×10^6/mL epimastigotes after incubation at 39 °C for 24 h. Reductase activity determined by MTT assay. **c** Mitochondrial membrane potential assay ($\Delta\Psi$m) was assayed with Rho 123 by flow cytometry using carbonyl cyanide 3-chloro phenylhydrazone (*CCCP*) as positive control and nonstressed parasites as negative control. **d** Apoptosis and necrosis assayed by flow cytometry using FITC Annexin V/Dead cell Apoptosis kit (Invitrogen). *b–d* result from three independent experiments. $^{***}P < 0.001$; $^{**}P < 0.01$. *Bar* = 1 μm

another biological parameter, we determined the rate of growth of the parasites after stress. Following the incubation in stress conditions, the cultures were diluted into fresh LIT broth to assess whether the cellular growth could be resumed. As shown in Fig. 6.2, when compared with control conditions, all the stress treatments affected the recovery of parasite growth, but with differences. The acidic and oxidative stress induced the lowest rate of growth recovery, with a growth rate of less of 20 %. In contrast, parasites exposed to nutritional stress or heat shock were able to grow at a rate of nearly 50 % compared with the control parasites.

Discussion

From the ecological point of view, infectious diseases are the result of the interactions between infectious microorganisms, hosts, vectors, and the ecosystem. In this process, some microorganisms like *T. cruzi* infect mammalian hosts, then pass to insects, where they can establish and then pass to the mammals again, thus adapting to different conditions in mammals and insects. *T. cruzi* colonizes the intestine of the hematophagous vector where it replicates as epimastigotes that later on will differentiate into the infective metacyclic trypomastigotes

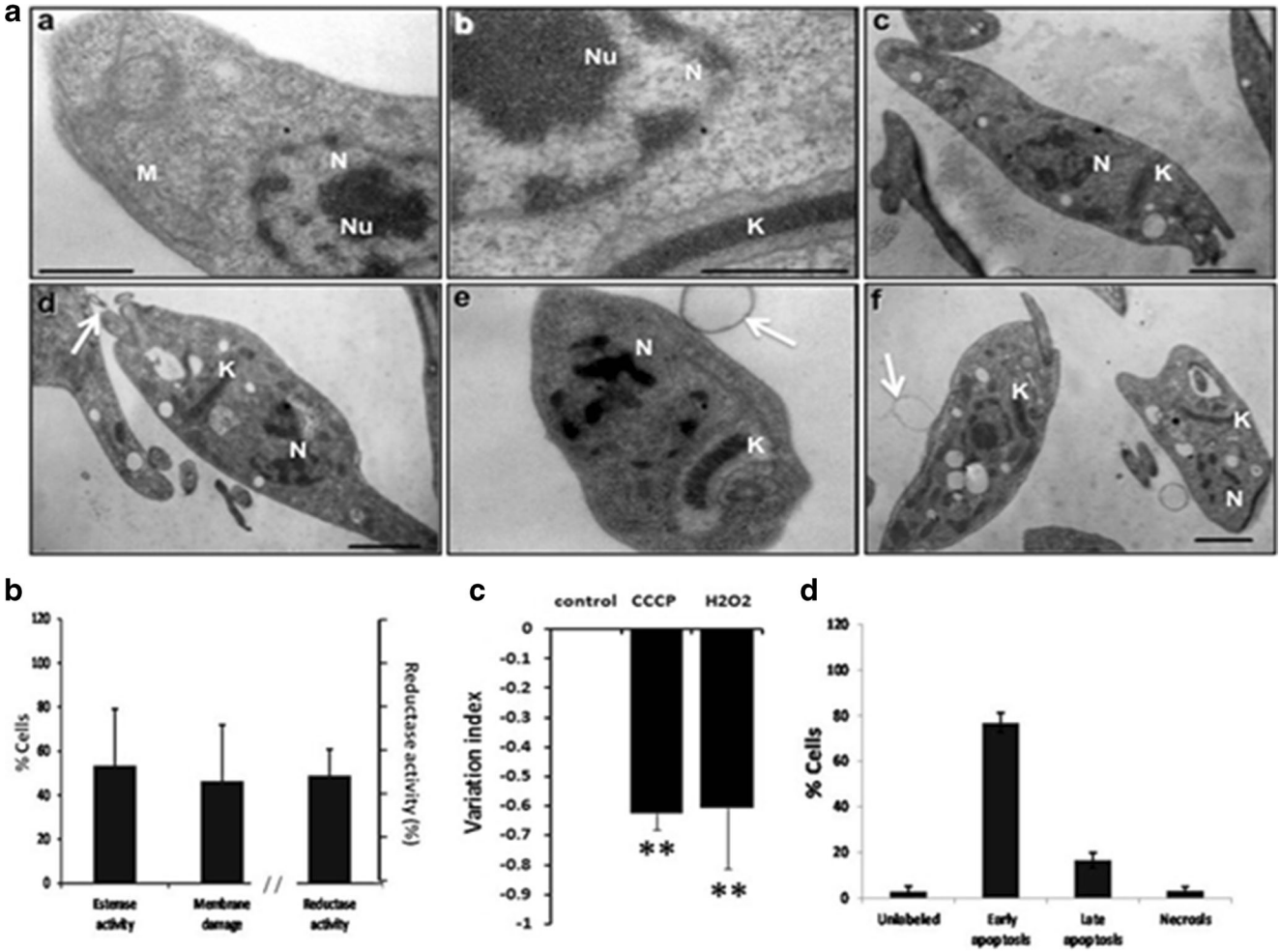

Fig. 5 Effects of oxidative stress on epimastigotes. **a** Representative transmission electron micrographs of *Trypanosoma cruzi* epimastigotes treated with oxidative stress (160 μM H_2O_2) for 2 h. **a** The ultrastructure of control parasites showing typical structure of nucleus (*N*), nucleolus (*Nu*), mitochondria (*M*), and kinetoplast (*K*) (*a* and *b*). **a** The ultrastructure of treated parasites exhibit an abnormal distribution of chromatin and absence of nucleolus (*c*–*e*, *N*), the formation of blebs in plasma membrane (*d*–*f*, *arrow*), and swelling of the mitochondria (*e*, *K*). **b** Esterase activity and plasma membrane integrity determined by LIVE/DEAD viability/cytotoxicity Kit (Molecular Probes) in 2×10^6/mL epimastigotes after incubation with 160 μM H_2O_2 for 2 h. Reductase activity determined by MTT assay. **c** Mitochondrial membrane potential assay (ΔΨm) was assayed with Rho 123 by flow cytometry using as positive control carbonyl cyanide 3-chloro phenylhydrazone (*CCCP*) and parasites no stressed as negative control. **d** Apoptosis and necrosis assayed by flow cytometry using FITC Annexin V/Dead cell Apoptosis kit (Invitrogen). **b**–**d** result from three independent experiments. $^{**}P < 0.01$. *Bar* = 1 μm

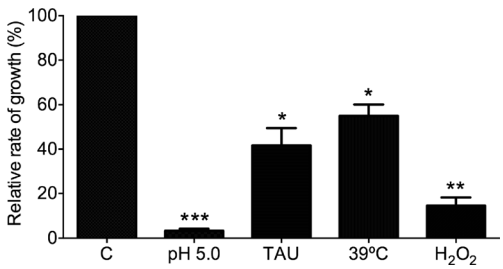

Fig. 6 Recovery of parasite growth after stress conditions. Two million control or stressed parasites (for 24 or 2 h as indicated in the text) per ml were reinoculated in fresh LIT medium, and after 48 h, the number of parasites was determined. The number of nonstressed control parasites was considered as 100 % of growth. Three independent experiments were done. $^{*}P < 0.05$; $^{**}P < 0.005$; $^{***}P < 0.0005$

form. During this cycle, they will confront different types of stress. Even though they are adapted to all these conditions, it is clear that they will suffer damage and their population can be diminished (Matthews 2011).

In this work, *T. cruzi* epimastigotes were subjected to different stress conditions, some of them similar to natural conditions and others as a study model with the aim to understand the morphological and metabolic responses to these conditions. All conditions were done in the Qro strain of the DTU TcI, which is the most conspicuous in Mexico, Central and South America. As many other microorganisms, *T. cruzi* presents a high genetic heterogeneity. The stress resistance has been shown to have intraspecies differences in *T. cruzi* (Dost

et al. 2004; Espinoza et al. 2010; Mielniczki-Pereira et al. 2007). Particularly, North American strains have been scarcely studied.

Acid, nutritional, temperature, and oxidative stress were applied to epimastigotes, and they were damaged in all the cases, but great differences were observed between the different types of stress. The acidic pH produced strong modifications in their morphology. They showed rounded forms and twisted bodies. There were also internal changes since there was an abnormal condensation of the chromatin and evident morphological alterations of the mitochondria. Surprisingly, a high percentage of the parasites were metabolically active as demonstrated by the metabolic assays that measured the esterase and reductase activities using the fluorescence of calcein and the MTT reduction assay, respectively. A moderated reduction of the $\Delta\Psi m$ was observed. The $\Delta\Psi m$ is essential for the maintenance of physiological functions of the respiratory chain, and the loss of $\Delta\Psi m$ reduce the cell energy production. This alteration has been related to the ROS presence and as a consequence the induction of cell death by apoptosis (Lazarin-Bidóia et al. 2016). In the experiments reported here, almost no parasites showed evidence of apoptotic or necrotic process. However, the morphological changes and the damage to the organelles correlate very well with the parasite incapacity to grow after the acidic stress was eliminated (Fig. 6).

During the acidic stress, the cells exposed to a high concentration of hydrogen ions are susceptible to loss the balance of different intra and extra cellular ions and then suffer from changes in the homeostasis of intracellular pH (Vieira 1998). Reports in *L. donovani* suggested that the loss of this homeostasis induces elimination of the membrane potential provoking an energetic collapse (Bera et al. 2003). Also, when *T. brucei* was subject to pH 5.5 during 2 h, their mobility, metabolism, and ATP levels were affected causing cell death (Nolan et al. 2000). In contrast, in our study, a strong metabolic activity was demonstrated by the esterase and reductase activities indicating different mechanisms to resist this kind of stress in the different kinetoplastids.

In this study, the parasites acquired a rounded form after the acidic pH, which can be a morphological adaptation to this type of stress. These morphological changes are associated to the metacyclogenesis and would explain the lack of growth of the parasites (Fig. 6). In bacteria, a similar phenomenon has been attributed to changes in the lipid composition of the bacterial membrane (Fozo and Quivey 2004; Mayorga-Reyes et al. 2009). In *T. cruzi*, the inhibition of ergoesterol synthesis, a membrane lipid, induces abnormal morphology of the parasite (Veiga-Santos et al. 2012). It will be interesting to study if there are any connections between acidic stress and changes in the membrane structure.

The nutritional stress did not produce a significant reduction on the parasite mobility. This contrasts with previous reports that showed reduction on this function (Martins et al. 2009), probably due to the different parasites strain used in the studies. In contrast, a clear reorganization of the morphology indicated by the reduction of the cellular area was observed (Fig. 1j). Also, numerous double membranes vacuoles were present, indicating an autophagy process. Similar results with nutritional stress were found by Alvarez and co-workers in the CL-Brener strain, a TcVI strain. These authors also demonstrate the presence of genes coding for proteins of the ATg8 conjugate system related to the autophagy process (Alvarez et al. 2008). In cells under nutritional stress, it is common to observe the process of autophagy, which consists in resisting the adverse condition by degrading diverse cellular components, including molecules and organelles. One of the characteristics of this phenomenon is the appearance of autophagosomes, double membrane vacuoles. These vacuoles then fuse with lysosomes, giving origin to autophagolysosomes, where the cellular components will be degraded. The autophagy is an important process for the maintenance of the metabolic balance, recycling of cellular components, and for the cell growth. Disequilibrium of this balance gives rise to cell death (Reggiori and Klionsky 2002).

For this type of stress, the esterase activity was not significantly affected, but the reductase activity was only 40 % of that of the control parasites. The $\Delta\Psi m$ was not different from the control parasites. But, growth was only 40 % from that showed by the control parasites. In contrast to previous reports, the autophagy phenomena indicated by the TEM experiments were not associated to a loss of membrane potential (Lazarin-Bidóia et al. 2013).

With relation to heat shock, there was no effect on the mobility of the parasites. However, important structural damage was observed at 39 °C during 24 h of incubation as an intense swelling in one section of the body. In similar studies using strains of different genetic background, inconsistent effects were found. When epimastigotes of the Maracay strain (TcVI) were incubated at 42 °C for 4 h, they got a round shape (Requena et al. 1992); nevertheless, with the same condition but using Silvio X10/4 strain (TcI), parasites were not affected (Olson et al. 1994). These data demonstrate once more the importance of the studies of stress damage using diverse types of stress and different genetic backgrounds of parasites. At a morphological level, the formation of stress granulates (Fig. 4a) has been described in different types of cells, from yeasts to eukaryotes (Souquere et al. 2009; Webster and Watson 1993). In *T. cruzi*, they have been detected by immunofluorescent studies and they were described as nontranscribed mRNA, since one of the effects observed during heat shock is the inhibition of transcription and translation process (Cassola et al. 2007; Názer et al. 2012). Other TEM observation was the presence of bubbles that has been reported when this parasite was treated with different drugs (Batista et al. 2010; Menna-Barreto et al. 2009a, b). These structures have been related to apoptosis in mammalian cells (Ricci and

Zong 2006). Also, apoptosis has been induced by heat shock in *L. amazonensis* (Moreira et al. 1996). In this study under heat-stress conditions, metabolic parameters were severely affected, including esterase and reductase activity as well as the $\Delta\Psi m$. Also, important membrane damage was observed by the incorporation of EthD-1 to the nuclear material. Surprisingly, this condition allowed the 55 % of the parasite grow recovery as indicated in Fig. 6. HSPs of high and low molecular weight have been implicated in protection against heat stress. Our group identified and characterized a small heat shock protein of 16 kDa (Pérez-Morales et al. 2009). It has been observed that this SHSP accumulates in the parasite during the heat shock at 39 °C for 24 h, suggesting its possible role for the survival of some parasites that could continue to grow. Currently, more studies with this protein are conducted in our laboratory.

T. cruzi has to contend with oxidative stress in many ways: its own metabolic products and the one produced by its invertebrate and mammals hosts. To defend from oxidative stress, *T. cruzi* has developed an unique enzymatic system, complex and effective: they have four isoforms of Fe-superoxide dismutase (Fe-SOD), peroxidase, peroxiredoxins, and they rely on trypanothione a specific trypanosomatid thiol (Piacenza et al. 2009; Wilkinson et al. 2002; Machado-Silva et al. 2016).

The parasite mobility was severely affected by the oxidative stress in a dose-dependent manner. Ultra-structural changes were observed, such as abnormal chromatine distribution and sometimes lack of nucleolus. Blebs in the membrane were observed indicating apoptosis, this late phenomenon was corroborated by damage to the membrane (Fig. 5b) and the PS translocation from the inner to the outer leaflet of the plasma membrane (Fig. 5c). Also, the esterase and reductase activity were affected. In accordance with all this damage, growth was severely affected. Comparable results were found using similar conditions (200 μM of H_2O_2), where after 2 h, the majority of the parasites were nonmobile (Finzi et al. 2004). In that work, an increase in tryparedoxin peroxidase activity was observed and the authors suggested an important role for this enzyme in the protection of the parasite to variant levels of ROS (Finzi et al. 2004). Our results on the processes of apoptosis during the oxidative stress (Fig. 5c) have also been reported in *L. donovani*, indicating a similar death process in these other Trypanosomatidae parasites (Das et al. 2001). Probably, autophagy was also present during oxidative stress since myelin-like structures were observed. It has been reported that these structures are present in cells suffering autophagy (Cyrino et al. 2012; Mofarrahi et al. 2012; Santos et al. 2010).

In summary, in this work, different effects of stress were observed in a TcI strain of *T. cruzi* with a diversity of damage in the parasite but with the possibility that important defense mechanisms like anti-oxidant pathways and HSPs of high and low molecular weight can act to protect the parasite and allow them to recover and still continue growing as in the case of nutritional and heat shock stress. This work, besides to contributing to the understanding of the effect of several types of stress in the same strain of *T. cruzi*, can also help to understand the observation of the different levels of resistance to drugs that has been reported in *T. cruzi*.

Acknowledgments This work was supported by DGAPA, UNAM, grant number IN206512. PMD received a scholarship from CONACYT during her PhD studies. We thank Dr. Ruben Arroyo-Olarte for his valuable comments and the help in the English review.

References

Alvarez EV, Kosec G, SantÁnna C, Turk V, Cazzulo JJ, Turk B (2008) Autophagy is involved in nutritional stress response and differentiation in *Trypanosoma cruzi*. J Biol Chem 283:3454–3464

Batista DG, Pacheco MG, Kumar A, Branowska D, Ismail MA, Hu L, Boykin DW, Soeiro MN (2010) Biological, ultrastructural effect and subcellular localization of aromatic diamidines in *Trypanosoma cruzi*. Parasitology 137:251–259

Bera A, Singh S, Nagaraj R, Vaidya T (2003) Induction of autophagic cell death in *Leishmania donovani* by antimicrobial peptides. Mol Biochem Parasitol 127:23–35

Carnieri EG, Moreno SN, Docampo R (1993) Trypanothione-dependent peroxide metabolism in *Trypanosoma cruzi* different stages. Mol Biochem Parasitol 61:79–86

Cassola A, De Gaudenzi JG, Frasch AC (2007) Recruitment of mRNAs to cytoplasmic ribonucleoprotein granules in trypanosomes. Mol Microbiol 65:655–670

Castillo JL, Reynolds SE, Eleftherianos I (2011) Insect immune responses to nematode parasites. Trends Parasitol 27:537–547

Chiari E, Camargo EP (1984) Culturing and cloning of *Trypanosoma cruzi*. In: Morel M (ed) Genes and Antigens of Parasite. Institute Oswaldo Cruz, Río de Janeiro, Brazil

Contreras VT, Salles JM, Thomas N, Morel CM, Goldenberg S (1985) *In vitro* differentiation of *Trypanosoma cruzi* under chemically defined conditions. Mol Biochem Parasitol 16:315–327

Cyrino LT, Araújo AP, Joazeiro PP, Vicente CP, Giorgio S (2012) *In vivo* and *in vitro Leishmania amazonensis* infection induces autophagy in macrophages. Tissue Cell 44:401–408

Das M, Mukherjee SB, Shaha C (2001) Hydrogen peroxide induces apoptosis-like death in *Leishmania donovani* promastigotes. J Cell Sci 114:2461–2469

de Souza W, Sant'Anna C, Cunha-e-Silva NL (2009) Electron microscopy and cytochemistry analysis of the endocytic pathway of pathogenic protozoa. Prog Histochem Cytochem 44(2):67–124. doi:10.1016/j.proghi.2009.01.001. Epub 2009 Apr 5

Dost CK, Saraiva J, Monesi N, Zentgraf U, Engels W, Albuquerque S (2004) Six *Trypanosoma cruzi* strains characterized by specific gene expression patterns. Parasitol Res 94:134–140

Espinoza B, Rico T, Sosa S, Oaxaca E, Vizcano-Castillo A, Caballero ML, Martínez I (2010) Mexican *Trypanosoma cruzi* TCI strains with different virulence induce diverse humoral and cellular immune response in murine experimental infection. J Biomed Biotech. doi:10.1155/2010/890672

Finzi JK, Chiavegatto CWM, Corat KF, López JA, Cabrera OG, Mielniczki-Pereia AA, Colli W, Alves MJM, Gadelha FR (2004) *Trypanosoma cruzi* response to the oxidative stress generated by hydrogen peroxide. Mol Biochem Parasitol 133:37–43

Fozo EM, Quivey RG Jr (2004) Shifts in the membrane fatty acid profile of *Streptococcus* mutans enhance survival in acidic environments. Appl Environ Microbiol 70:929–936

Grela E, Ząbek A, Grabowiecka A (2015) Interferences in the Optimization of the MTT Assay for Viability Estimation of *Proteus mirabilis*. Avicenna J Med Biotechnol 7:159–167

Hall BF (1993) *Trypanosoma cruzi*: mechanisms for entry into host cells. Sem Cell Biol 4:323–333

Jiménez-García LF, Segura-Valdéz ML (2004) Visualizing nuclear structure *in situ* by atomic force microscopy. Meth Mol Biol 242:191–199

Kollien A, Schaub GA (1998) *Trypanosoma cruzi* in the rectum of the bug *Triatoma infestans*: effects of blood ingestion by the starved vector. Am J Trop Med Hyg 59:166–170

Kollien AH, Grospietsch T, Kleffmann T, Zerbst-Boroffka I, Schaub GA (2001) Ionic composition of the rectal contents and excreta of the reduviid bug *Triatoma infestans*. J Insec Physiol 47:739–747

Lazarin-Bidóia D, Desoti VC, Ueda-Nakamura T, Dias Filho BP, Nakamura CV, Silva SO (2013) Further evidence of the trypanocidal action of eupomatenoid-5: confirmation of involvement of reactive oxygen species and mitochondria owing to a reduction in trypanothione reductase activity. Free Rad Biol Med 60:17–28

Lazarin-Bidóia D, Desoti VC, Martins SC, Ribeiro FM, Ud Din Z, Rodrigues-Filho E, Ueda-Nakamura T, Nakamura CV, de Oliveira Silva S (2016) Dibenzylideneacetones are potent trypanocidal compounds that affect the *Trypanosoma cruzi* redox system. Antimicrob Agents Chemother 60:890–903

Machado-Silva A, Cerqueira PG, Graziell-Silva V, Gadelha FR, Peloso-Ede F, Teixeira SM, Machado CR (2016) How *Trypanosoma cruzi* deals with oxidative stress: antioxidant defense and DNA repair patways. Mutat Res Rev Mutat Res 767:8–22

Martins RM, Covarrubias C, Rojas RG, Silber AM, Yoshida N (2009) Use of L-proline and ATP production by *Trypanosoma cruzi* metacyclic forms as requirements for host cell invasion. Infec Imm 77:3023–3032

Matthews KR (2011) Controlling and coordinating development in vector-transmitted parasites. Science 331:1149–1153

Mayorga-Reyes L, Bustamante-Camilo P, Gutiérrez-Nava A, Barranco-Florido E, Azaola-Espinosa A (2009) Crecimiento, sobrevivencia y adaptación de *Bifidobacterium infantis* a condiciones ácidas. Revista Mexicana de Ingeniería Química 8:259–264

Menna-Barreto RF, Corrêa JR, Cascabulho CM, Fernandes MC, Pinto AV, Soares MJ, De Castro SL (2009a) Naphthoimidazoles promote different death phenotypes in *Trypanosoma cruzi*. Parasitology 136:499–510

Menna-Barreto RF, Salomão K, Dantas AP, Santa-Rita RM, Soares MJ, Barbosa HS, de Castro SL (2009b) Different cell death pathways induced by drugs in *Trypanosoma cruzi*: an ultrastructural study. Micron 40:157–168

Mielniczki-Pereira AA, Chiavegatto CM, López JA, Colli W, Alves MJ, Gadelha FR (2007) *Trypanosoma cruzi* strains, Tulahuen 2 and Y, besides the difference in resistance to oxidative stress, display differential glucose-6-phosphate and 6-phosphogluconate dehydrogenases activities. Acta Trop 101:54–60

Mofarrahi M, Sigala I, Guo Y, Godin R, Davis EC, Petrof B, Sandri M, Burelle Y, Hussain SN (2012) Autophagy and skeletal muscles in sepsis. PLoS One 7:e47265

Moreira ME, Del Portillo HA, Milder RV, Balanco JM, Barcinski MA (1996) Heat shock induction of apoptosis in promastigotes of the unicellular organism *Leishmania* (*Leishmania*) *amazonensis*. J Cell Physiol 167:305–313

Názer E, Verdún RE, Sánchez DO (2012) Severe heat shock induces nucleolar accumulation of mRNAs in *Trypanosoma cruzi*. PLoS One 7:e43715

Nogueira NP, Saraiva FMS, Sultano PE, Cunha PRBB, Laranja GAT, Justo GA, Sabino KCC, Coelho MGP, Rossini A, Atella GC, Paes MC (2015) Proliferation and differentiation of *Trypanosoma cruzi* inside its vector have a new trigger: redox status. Plos One. doi:10.1371/journal.pone.0116712

Nolan DP, Rolin S, Rodriguez JR, Van Den Abbeele J, Pays E (2000) Slender and stumpy bloodstream forms of *Trypanosoma brucei* display a differential response to extracellular acidic and proteolytic stress. Eur J Biochem 267:18–27

Olson CL, Nadeau KC, Sullivan MA, Winquist AG, Donelson JE, Walsh CT, Engmann DM (1994) Molecular and biochemical comparison of the 70-kDa heat shock proteins of *Trypanosoma cruzi*. J Biol Chem 269:3868–3874

Pérez-Morales D, Ostoa-Saloma P, Espinoza B (2009) *Trypanosoma cruzi* SHSP16: characterization of an α-crystallin small heat shock protein. Exp Parasitol 123:182–189

Piacenza L, Alvarez MN, Peluffo G, Radi R (2009) Fighting the oxidative assault: the *Trypanosoma cruzi* journey to infection. Curr Opinion Microbiol 12:415–421

Piacenza L, Peluffo G, Alvárez MN, Martínez A, Radi R (2013) *Trypanosoma cruzi* antioxidant enzymes as virulent factors in Chagas Disease. Antox Redox Signal 19:723–734

Raff M (1998) Cell suicide for beginners. Nature 396:119–122

Reggiori F, Klionsky DJ (2002) Autophagy in the eukaryotic cell. Euk Cell 1:11–21

Requena JM, Jimenez-Ruiz A, Soto M, Assiego R, Santarén JF, López MC, Patarroyo ME, Alonso C (1992) Regulation of hsp70 expression in *Trypanosoma cruzi* by temperature and growth phase. Mol Biochem Parasitol 53:201–212

Ricci MS, Zong WX (2006) Chemotherapeutic approaches for targeting cell death pathways. Oncologist 11:342–357

Sandes JM, Fontes A, Regis-da-Silva CG, de Castro MCAB, Lima-Junior CG, Silva FPL et al (2014) *Trypanosoma cruzi* cell death induced by the Morita-Baylis-Hillman adduct 3-Hydroxy-2-Methylene-3-(4-Nitrophenylpropanenitrile). PLoS One 9(4):e93936

Santos AO, Santin AC, Yamaguchi MU, Cortez LE, Ueda-Nakamura T, Dias-Filho BP, Nakamura CV (2010) Antileishmanial activity of an essential oil from the leaves and flowers of *Achillea millefolium*. Ann Trop Med Parasitol 104:475–483

Souquere S, Mollet S, Kress M, Dautry F, Pierron G, Weil D (2009) Unravelling the ultrastructure of stress granules and associated P-bodies in human cells. J Cell Sci 122:3619–3626

Thammavongs B, Denou E, Missous G, Guéguen M, Panoff JM (2008) Response to environmental stress as a global phenomenon in biology: the example of microorganisms. Micro Environ 23:20–23

Vassar Stats: Statistical computational Web site. http://vassarstats.net/

Veiga-Santos P, Barrias ES, Santos JF, de Barros Moreira TL, de Carvalho TM, Urbina JA, de Souza W (2012) Effects of amiodarone and posaconazole on the growth and ultrastructure of *Trypanosoma cruzi*. Inter. J. Antimicrobial Agents 40:61–71

Vieira LL (1998) pH and volume homeostasis in trypanosomatids: current views and perspectives. Biochim Biophys Acta 1376:221–224

Volpato H, Desoti VC, Valdez RH, Ueda-Nakamura T, Silva SO, Sarragiotto MH et al (2015) Mitochondrial Dysfunction Induced by *N*-Butyl-1-(4-Dimethylamino) Phenyl-1, 2,3,4-Tetrahydro-β-Carboline-3-Carboxamide Is Required for Cell Death of *Trypanosoma cruzi*. PLoS One 10(6):e0130652. doi:10.1371/journal.pone.0130652

Webster DL, Watson K (1993) Ultrastructural changes in yeast following heat shock and recovery. Yeast 9:1165–1175

Weis VM (2008) Cellular mechanisms of Cnidarian bleaching: stress causes the collapse of symbiosis. J Exp Biol 211:3050–3060

WHO (2015) Chagas disease. (http://www.who.int/mediacentre/factsheets/fs340/en/). Accessed on September 4th, 2015.

Wilkinson SR, Taylor MC, Touitha S, Mauricio IL, Meyer D, Kelly J (2002) TcGPXII a glutathione-dependent *Trypanosoma cruzi* peroxidase with substrate specificity restricted to fatty acid and phospholipid hydroperoxides is localized to the endoplasmic reticulum. Biochem J 364:787–794

Wyllie AH, Kerr JFK, Currie AR (1980) Cell death. The significance of apoptosis. Inf Rev Cytol 68:251–306